ACADEMIA ROMÂNĂ
Revue Roumaine de Chimie
http://web.icf.ro/rrch/

Rev. Roum. Chim.,
2015, *60*(5-6), 467-475

ELECTROCHEMICAL OXIDATION MECHANISM OF ANTICANCER DRUG NILOTINIB

Burcu DOGAN-TOPAL, Burcin BOZAL-PALABIYIK, Sibel A. OZKAN and Bengi USLU*

Ankara University, Faculty of Pharmacy, Department of Analytical Chemistry, 06100 Tandogan, Ankara, Turkey

Received November 17, 2014

The kinetics and mechanism for electrochemical oxidation of Nilotinib, a tyrosine kinase inhibitor drug, used in the treatment of chronic myelogenous leukemia, were studied using cyclic and differential pulse voltammetric methods on glassy carbon electrode. The pH-dependent oxidation of Nilotinib was studied within the range of pH 0.3-10.0. Two well-defined peaks were observed, 1.09 V, and 1.44 V (versus Ag/AgCl) in phosphate buffer at pH 2.0 by differential pulse voltammetry. The irreversible and mixed diffusion-adsorption controlled electrochemical oxidation of Nilotinib was revealed by studies at different scan rates. The rate constant, surface coverage coefficients of adsorbed molecules and the number of electrons transferred in electrode mechanisms were calculated. The mechanism was evaluated with model compounds having the diphenylamine moiety and acetamide group in their structure. The oxidation processes for two anodic peaks were found to be two-electron transfers.

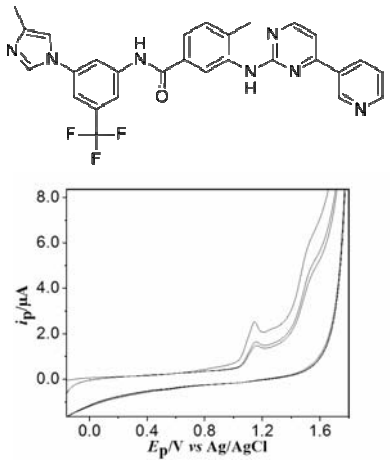

INTRODUCTION

Electrochemical studies furnish an enormous amount of evidence regarding the mechanisms of biological electron-transfer processes.[1] Electrochemistry has always provided analytical methods characterized by instrumental simplicity, moderate cost, and portability. Cyclic voltammetry (CV) is the most widely used voltammetric technique and it is important in the initial stages of developing and optimizing a particular electroanalytical method. This method gives the qualitative information about electrochemical reactions. Actually, from the peak currents or peak heights, the power of cyclic voltammetry results from its ability to rapidly provide considerable information on the thermodynamics of redox processes and the kinetics of heterogeneous electron transfer reactions and on coupled chemical reactions or adsorption processes.[2-4] A pulse technique was proposed in order to increase the sensitivity of the technique. Differential pulse voltammetry (DPV) has been extremely useful for the determination of trace amounts of electroactive compound in pharmaceuticals. In our study, the differences of two voltammetric techniques were seen in pH dependency studies of drug.

In electrochemical studies, the glassy carbon (GC) is the most common carbon-based working electrodes into the redox mechanism of pharmaceutically active compounds. GC has a structure that is more closely related to that of a glassy material, with high luster and glass-like fracture characteristics, hence the name glassy (or

* Corresponding author: buslu@pharmacy.ankara.edu.tr , tel: +903122033178, fax: +90 312 2031081

vitreous).[5] GC, is a class of non graphitizing carbon, consisted of pure carbon combining glass-like mechanic characteristics with physical properties of graphite. It has some remarkable properties, such as high strength, high resistance to chemical attack and extreme impermeability to gases and liquids. According to the general specifications, GC is similar to polycrystalline graphite in composition, bonding and resistance, but differs greatly in porosity, low density, high robustness, high strength, good electrical conductivity and mechanical properties, all due to the difference in structure caused by the origin of each material.

Hence, the electrochemical technique can be used for clarifying and understanding the redox mechanisms of many biologically significant molecules and pharmaceutically active compounds.[1] Nilotinib (NLT) (Scheme 1a), in the form of the hydrochloride monohydrate salt, is a small molecule, a tyrosine kinase inhibitor approved for the treatment of imatinib-resistant chronic myelogenous leukemia[6]. NLT is an orally bioavailable derivative of imatinib with improved specificity toward the breakpoint cluster region-Abelson murine leukemia *(bcr-abl)* viral protooncogene.[7]

To our best knowledge, there is no literature on the anodic voltammetric behaviour of NLT. Information on the oxidation mechanism of NLT was obtained from results at different pH values may enable the clarification and improvement of the overall knowledge of the physiological mechanisms of action of NLT.

In this study, the electrochemical oxidation mechanism of NLT was studied in detail on GCE based on pH, scan rate and model compounds studies by CV. The rate constant, surface coverage coefficients of adsorbed molecules and the numbers of electrons transferred in electrode mechanisms were evaluated.

RESULTS AND DISCUSSION

No previous detailed electrochemical data were available concerning the electrode behaviour of NLT. In this study electrochemical mechanism of NLT was evaluated by means of pH dependency by CV and DPV techniques and scan rate studies.

pH dependency by DPV

The pH is an important factor in the electrochemical behaviour of organic compounds because protons are always involved in the electrochemical reactions and exert a significant impact on the reaction speed. Shifting in the peak potential with pH was considered as a proof of existence of protons in oxidation mechanism. The pH-dependent oxidation of NLT was studied within the range of pH 0.3-10.0. As seen in Fig. 1, NLT exhibited two main anodic peaks, at 1.09 V (first peak), and at 1.44 V (second peak) in pH 2.0 phosphate buffer by DPV. After pH 2.5, the first peak of NLT gave a shoulder and then with pH 5.7, this shoulder disappeared.

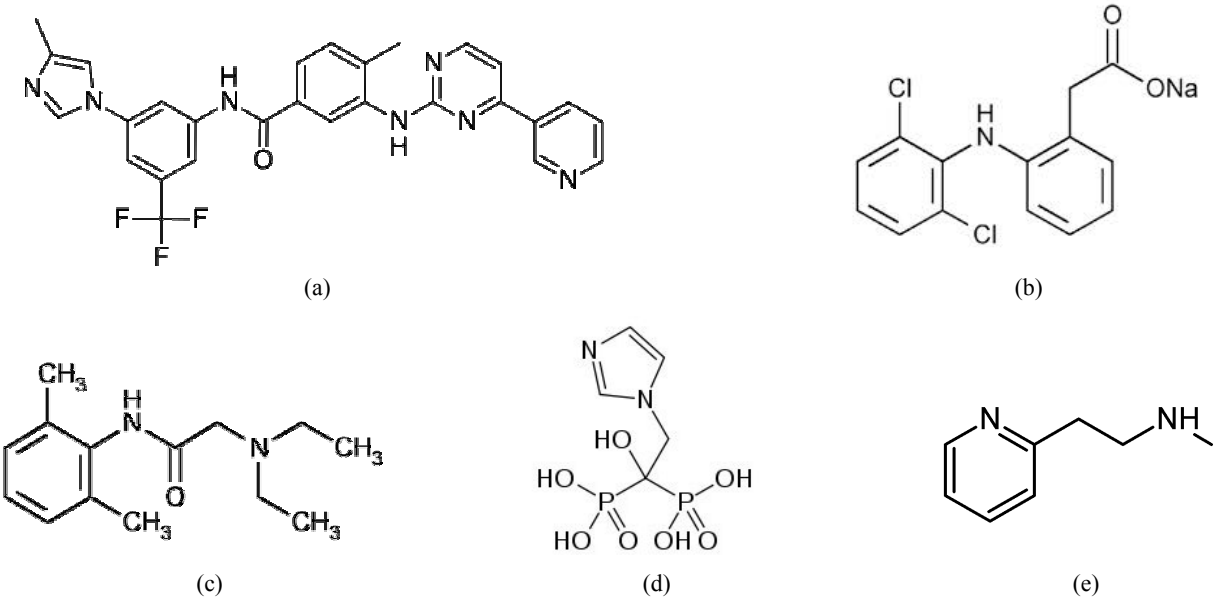

Scheme 1 – Structure of Nilotinib (a), Diclofenac (b), Lidocaine (c), Zoledronic acid (d), Betahistin (e).

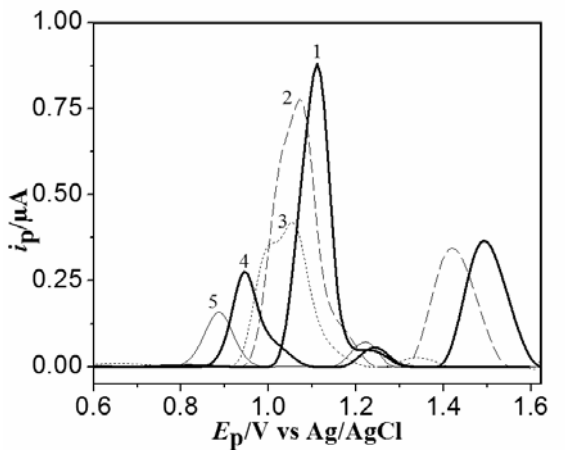

Fig. 1 – DP voltammograms of 10 μg mL^{-1} NLT solution on different pH values as pH 1.5 phosphate buffer (1); pH 2.5 phosphate buffer (2); pH 3.7 acetate buffer (3); pH 5.7 acetate buffer (4); pH 8.0 phosphate buffer (5).

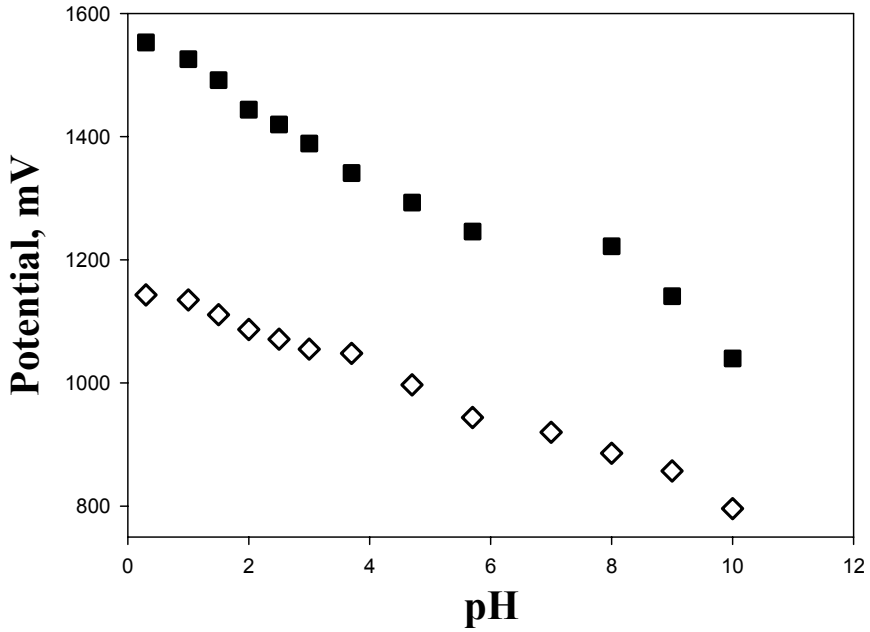

Fig. 2 – E_p-pH plot of 10 μg mL^{-1} NLT obtained by DPV in various buffer solutions and pH values; the first peak (◊) and the second peak (■).

By DPV, as seen in Fig. 2, the peak potentials of NLT shifted to less positive potentials with increasing pH. The plot of the peak potential (E_p) versus pH by DPV showed straight lines for the first and second peaks, which can be expressed by the following equations:

$$E_{p1} = 1162.2 - 35.25\ \text{pH};\ r = 0.996\ (\text{pH } 0.3\text{-}10.0)\ \text{for the first peak} \quad (1)$$

$$E_{p2} = 1572.4 - 59.33\ \text{pH};\ r = 0.996\ (\text{pH } 0.3\text{-}5.7)\ \text{first inclement for the second peak} \quad (2)$$

$$E_{p2} = 1953.3 - 91\ \text{pH};\ r = 0.998\ (\text{pH } 8.0\text{-}10.0)\ \text{second inclement for the second peak} \quad (3)$$

As it is seen above, the second peak was observed after pH 5.7 by DPV. For the second peak, the two intersection points and two inclements were seen in Eq. 2 and 3 (Fig. 2). The potential was independent from pH in the range of 5.7 - 8.0. For the second peak, the intersection of 5.7, is close to the pK_a value of NLT which is 5.68.[8] Thus the observed pH dependence indicates that the electroactive group, which is corresponding to the second peak, is in acid-base equilibrium with pK_a about 5.68.

pH dependency by CV

The results of CV investigations into the redox mechanism of pharmaceutically active compounds and biomolecules may have profound effects on understanding their in vivo redox processes or pharmaceutical activity. The repetitive cyclic voltammograms of 10 μg mL^{-1} NLT could be seen at GCE in phosphate buffer at pH 2.0 in Fig. 3. As seen in Fig. 3a, NLT exhibited two main anodic peaks, at 1.15 V (the first peak), and at 1.52 V (the second peak), one anodic wave, at 1.26 V, also one cathodic peak at 0.55 V. After the first cycle, new peaks emerged at 0.62 V and 0.80 V on the anodic branch. In further successive cyclic voltammograms, while the two anodic peak currents decreased, the newly emerged peak current enhanced and peak potential shifted to 0.63 V. On the anodic branch, in order to find which main peak is responsible for the new peaks that occurred, two different potential ranges were determined as working range. Fig. 3b shows first and third cycles of different potential ranges. In this figure, from –0.2 V to 1.23 V (solid line), the new peaks were distinctly seen, while this new peak was seen as a wave when initial potential was 1.35 V (dashed line). Also, Fig. 3b was zoomed, it was shown as Fig. 3c; when end potential is 1.23 V (solid line), two anodic (0.577 V and 0.79 V) and one cathodic peak (0.528 V) were distinctly obtained in pH 2.0 phosphate buffer. These redox couple and irreversible new peaks were formed due to reaction of the NLT oxidation product at the GCE surface during the first scan. These product peaks may explain the hydroxyl derivatives of NLT oxidation (Scheme 2).

In Fig. 3b, the decrease in the currents of the first and second peaks was observed on the second scan. It could be explained by the adsorption of NLT oxidation products at the electrode surface, as seen Fig. 3c.

The concentration of NLT adsorbed onto the GCE surface in pH 2.0 phosphate buffer solutions was calculated from the following equation for only the second peak with adsorption behaviour:[9,10]

$$\Gamma_{NLT}=Q\,(nFA)^{-1} \qquad (4)$$

where n is the number of electrons transferred in electrode reaction; Γ is the surface coverage of adsorbed substance (mol cm^{-2}); A is the working GC electrode area (0.02 cm^{-2}), F is the Faraday constant (96485 C mol) and where the charge Q, from the area under the peak. The Γ_{NLT} was found as 2.98×10^{-11} mol cm^{-2} for second peaks.

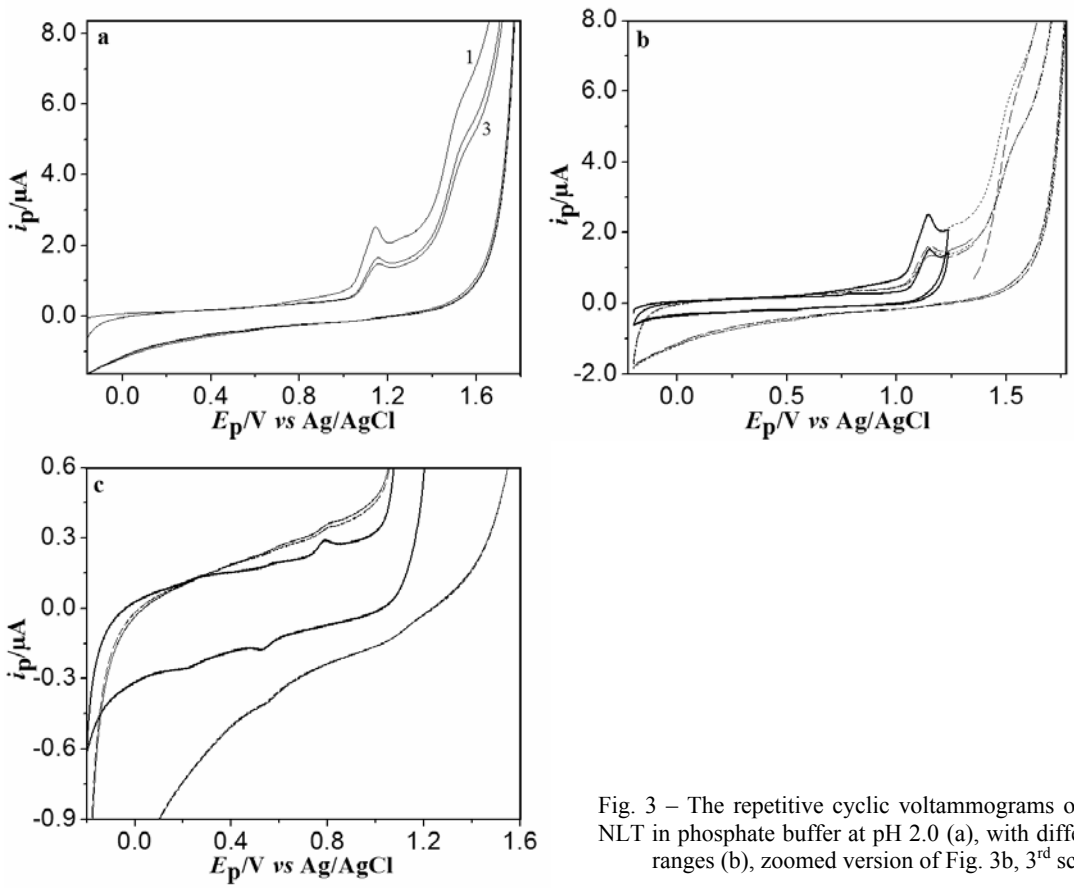

Fig. 3 – The repetitive cyclic voltammograms of 20 μg mL^{-1} NLT in phosphate buffer at pH 2.0 (a), with different potential ranges (b), zoomed version of Fig. 3b, 3rd scan (c).

Also, the peak potentials of NLT shifted to less positive potentials with increasing pH by CV. As seen in Fig. 4, the plot of the peak potential (E_p) versus pH showed straight lines for the first and second peaks, which can be expressed by the following equations:

$$E_{p1} = 1271.1 - 34.17\ \text{pH};\ r = 0.995\ (\text{pH } 0.30\text{-}10.0)\ \text{for the first peak;} \quad (5)$$

$$E_{p2} = 1639.3 - 61.76\ \text{pH};\ r = 0.994\ (\text{pH } 0.3\text{-}5.70)\ \text{for the second peak.} \quad (6)$$

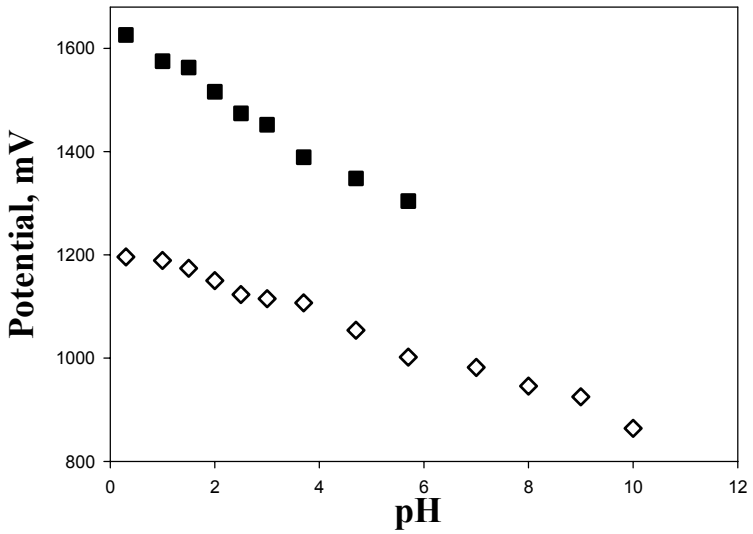

Fig. 4 – E_p-pH plot of 10 μg mL^{-1} NLT obtained by CV in various buffer solutions and pH values; the first peak (◊) and the second peak (■).

The slope of E_p *vs.* pH corresponds to 34.17 mV/pH and 61.76 mV/pH for the first peak and second peak, respectively. The second peak disappeared after pH 5.7 (different from DPV).

When the slope of this relation was evaluated in Eq. 7, the ratio of proton to electron participated in:

$$E_p = E^o - \left(\frac{2.303RTm}{\alpha nF}\right)\text{pH} \quad (7)$$

where α is the transfer electron coefficient, m is the number of protons involved in the reaction, and the other symbols connote their usual meanings.[11] The slope values indicated above show that in the first peak oxidation process, the number of protons transferred is half of the number of electrons whereas in the second peak oxidation process, the number of protons is equal to the number of electrons.

Scan rate studies

More detailed experimental studies were carried out about characteristic of NLT oxidation by CV. The scan rate studies between 0.005 and 0.5 V s^{-1} were carried out to state whether the two oxidation processes on GCE were under diffusion or adsorption-controlled in 10 μg mL^{-1} NLT solutions. The equations are given below for two oxidation peaks in 0.5 M sulphuric acid by CV:

for the first peak;

$$i_{p1}\ (\mu\text{A}) = 8.63\ v\ (\text{V s}^{-1}) + 0.20\ (r = 0.999)\ \text{and} \quad (8)$$

$$\log i_{p1}\ (\mu\text{A}) = 0.75 \log v\ (\text{V s}^{-1}) + 0.82\ (r = 0.997) \quad (9)$$

for the second peak;

$$i_{p2}\ (\mu\text{A}) = 2.63\ v\ (\text{V s}^{-1}) + 0.05 \quad (r = 0.996)\ \text{and} \quad (10)$$

$$\log i_{p2}\ (\mu\text{A}) = 0.86 \log v\ (\text{V s}^{-1}) - 2.17\ (r = 0.995) \quad (11)$$

The log i_{p1} – log v and log i_{p2} – log v slopes were found as 0.75 and 0.86, respectively. According to these results, for both peaks, the electrochemical reactions were found as diffusion-adsorption mixed controlled process.[12]

The two oxidation peak potentials shifted to more negative potential values with the increase in the scan rates. As could be seen in the equations, peak potential shifted to more anodic values with increasing scan rate confirming and supporting the irreversibility. The linear relation between peak potential and logarithm of scan rate can be expressed by the following equations, for the first peak;

$$E_{p1}\ (\text{V}) = 1.20 + 0.02 \log v\ (\text{V s}^{-1}),\ (r = 0.999) \quad (12)$$

for the second peak;

$$E_{p2}\,(\mathrm{V}) = 1.48 + 0.05 \log v\ (\mathrm{V\ s^{-1}}),\ (r = 0.992)\ \text{first inclement}\ (0.075\text{-}0.5\ \mathrm{V\ s^{-1}}) \quad (13)$$

$$E_{p2}\,(\mathrm{V}) = 1.53 + 0.03 \log v\ (\mathrm{V\ s^{-1}}),\ (r = 0.990)\ \text{second inclement}\ (0.005\text{-}0.2\ \mathrm{V\ s^{-1}}) \quad (14)$$

For irreversible systems the peak potential of an anodic process shifted towards more positive potentials by about $30/\alpha n_\alpha$ mV for a tenfold increase in the scan rate.[9, 13, 14] α is the anodic charge transfer coefficient, n the number of electrons in the rate-determining step. In the scan rate range 0.005 - 0.5 V s^{-1}, the potential values shifted as 26 mV and 25 mV for the first and second peak, respectively. Hence αn_α values were calculated as 1.15 and 1.20 for the first and second peak, respectively. In most systems α turns out to lie between 0.3 and 0.7, and it can usually be assumed to be 0.5 in organic electrode reactions, but clearly this is only a rough approximation. Therefore, the values of n = 2.30 and 2.40 (~2) were obtained for the first and second peak, respectively. Based on pH dependency on potential by CV, two electrons and one proton were transferred for the first peak, and two electrons and two protons were calculated for the second peak oxidation process.

To understand the effect of pH on scan rate, also, in pH 2.0 phosphate buffer within 20 µg mL^{-1} NLT solutions by CV, the equations of scan rate studies were given again for two oxidation peaks: for the first peak;

$$i_{p1}\,(\mu\mathrm{A}) = 6.30\ v\ (\mathrm{V\ s^{-1}}) + 0.25\ (r = 0.994)\ \text{and} \quad (15)$$

$$\log i_{p1}\,(\mu\mathrm{A}) = 0.76 \log v\ (\mathrm{V\ s^{-1}}) + 0.75\ (r = 0.999) \quad (16)$$

for the second peak;

$$i_{p2}\,(\mu\mathrm{A}) = 5.060\ v\ (\mathrm{V\ s^{-1}}) - 0.001 \quad (r = 0.992)\ \text{and} \quad (17)$$

$$\log i_{p2}\,(\mu\mathrm{A}) = 1.00 \log v\ (\mathrm{V\ s^{-1}}) + 0.70\ (r = 0.992) \quad (18)$$

The slopes of log i_p – log v were found as 0.76 and 0.99, respectively. According to these results, the electrochemical reactions were found as diffusion-adsorption mixed for the first and adsorption controlled process for the second peak.[12]

The two oxidation peak potentials shifted to more negative potential values confirming and supporting the irreversibility with the increase in the scan rates. The linear relation between peak potential and logarithm of scan rate can be expressed by the following equations, for the first peak;

$$E_{p1}\,(\mathrm{V}) = 1.17 + 0.03 \log v\ (\mathrm{V\ s^{-1}}),\ (r = 0.997) \quad (19)$$

for the second peak;

$$E_{p2}(\mathrm{V}) = 1.57 + 0.06 \log v\ (\mathrm{V\ s^{-1}}),\ (r = 0.996) \quad (20)$$

In order to determine the heterogeneous electron-transfer rate constant (k^o) for the NLT second oxidation peak (which is compatible with the Laviron equation) on the GCE, cyclic voltammetric experiments were performed at different scan rates regarding the Laviron equation.[15]

$$Ep = E^{0\prime} - \left(\frac{2.303RT}{\alpha nF}\right)\log\left(\frac{RTk^0}{\alpha nF}\right) + \left(\frac{2.303RT}{\alpha nF}\right)\log\nu \quad (21)$$

where $E^{0\prime}$ is the formal potential, T is the temperature in degrees Kelvin, α=0.5 is the transfer coefficient, k^o is the rate constant for the interfacial electron transfer process, n=2 is the number of electrons transferred in the rate determining step, v is the scan rate, F is the Faraday constant, and R is the universal gas constant. The value of E^0= 1.468 V were obtained from the intercepts of a plot of E_p versus v at GCE for second peak. From this, k^o was calculated to be 0.814 s^{-1} in pH 2.0 phosphate buffer solution.

Electrochemical oxidation mechanism

Voltammetric methods, especially the CV, are most suitable for investigating the redox behavior of the new pharmaceutical compound and for enlightening its metabolic behaviour.[1, 16, 17] The anodic oxidative behavior of NLT is comparable to diphenylamine and phenyl acetamide oxidations that were reported in the literature assay.[18, 19] To support the working hypothesis, the diphenylamine moiety and acetamide group in NLT molecule structure that undergoes oxidation, the electrochemical behavior of NLT was compared with some model compounds. There are two main groupings present in the structure of NLT, which might be considered as undergoing electro-oxidation: the diphenylamine and acetamide group.[16, 17] Diclofenac and lidocaine were used as model substances for oxidation of the diphenylamine and the acetamide group moieties, respectively.

The oxidation of acetamide group moiety in lidocaine strongly indicate that the NLT second oxidation step is related to the amine moiety on the acetamide structure (Fig 5a). In the Ref. 18, the slope of E_p *vs.* pH was found as 52 mV/pH which was close to our results. The pK_a of the lidocaine was also investigated by means of plot peak potentials *vs.* pH. The value of 7.68 was found using the intersection of the two linear curves observed in this literature.

Our obtained results revealed a good agreement with the redox mechanism postulated for the model compound, diclofenac, by oxidation on the nitrogen atom in the diphenylamine moiety of the NLT molecule (Fig. 5b). As seen in the literature,[19] the potentials shifted negatively with increasing pH (in the range of 1-9) with the slope of 37 mV. In this pH range, two electrons and one proton are involved in electrochemical reaction. These results are compatible with the findings of this study, and they strongly indicate that the NLT first oxidation step is related to the amine moiety on the pyrimidin-phenylamine structure.

In addition, zoledronic acid and betahistine were studied as model compounds, for the imidazole and pyridine moieties in the NLT structure, respectively. But no peak appeared for both model compounds in our experimental conditions.

Based on these results, a possible oxidation mechanism was proposed in Scheme 2. As seen in Scheme 2, the diphenylamine and acetamide group in the molecule were given hydroxyl product. This product was seen in both oxidizible group that could be explained within the repetitive cyclic voltammograms (Figs. 3c and 5).

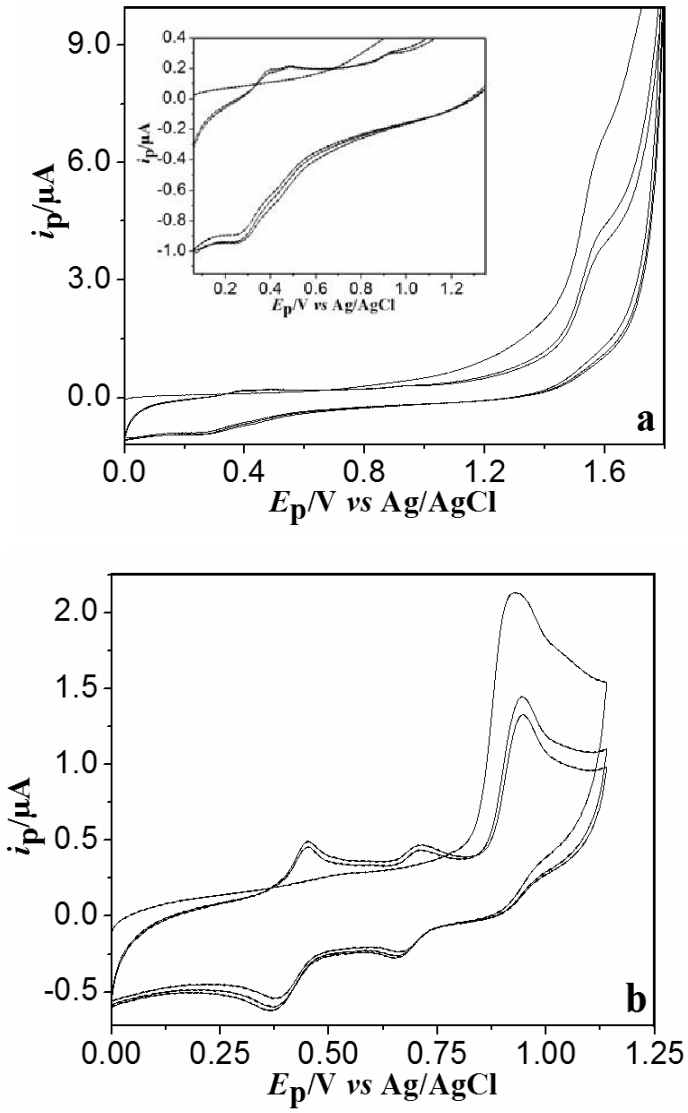

Fig. 5 – By repetitive cyclic voltammograms in 0.1 M H_2SO_4 40 ppm lidocaine (a), 20 ppm diclofenac (b) by 100 mV s^{-1}.

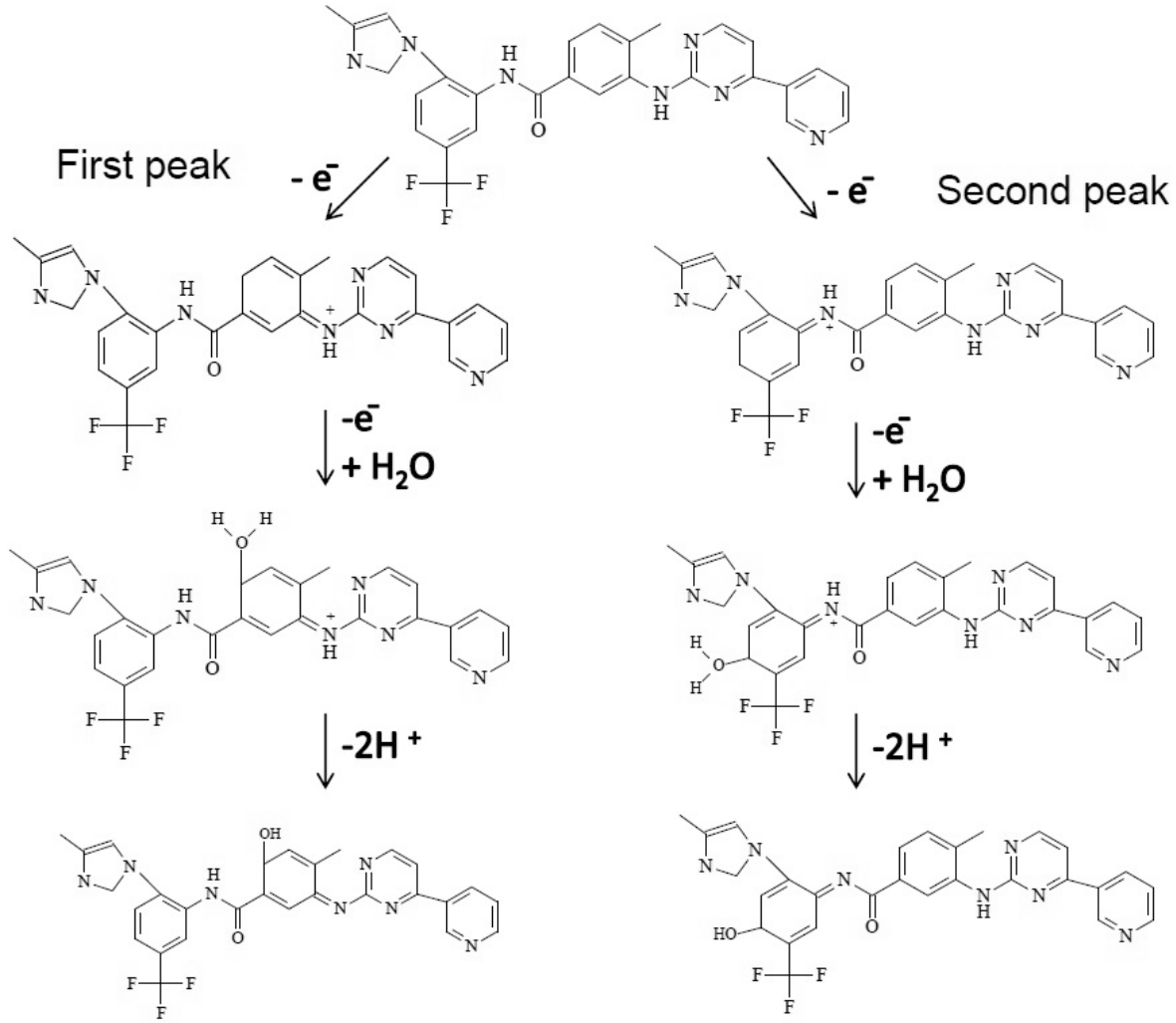

Scheme 2 – Possible oxidation pathway of NLT.

Table 1

Supporting electrolytes

pH	Acid	Base
0.3	0.5 M H_2SO_4	-
1.0	0.1 M H_2SO_4	-
1.5	0.315 M H_3PO_4	0.1 M $NaH_2PO_4.2H_2O$
2.0	0.1 M H_3PO_4	0.1 M $NaH_2PO_4.2H_2O$
2.5	0.0315 M H_3PO_4	0.1 M $NaH_2PO_4.2H_2O$
3.0	0.01 M H_3PO_4	0.1 M $NaH_2PO_4.2H_2O$
3.7	0.25 M CH_3COOH	0.025 M $CH_3COONa.3H_2O$
4.7	0.1 M CH_3COOH	0.1 M $CH_3COONa.3H_2O$
5.7	0.025 M CH_3COOH	0.25 M $CH_3COONa.3H_2O$
7.0	0.06 M $NaH_2PO_4.2H_2O$	0.1 M Na_2HPO_4
8.0	0.01 M $NaH_2PO_4.2H_2O$	0.16 M Na_2HPO_4
9.0	0.15 M H_3BO_3	0.05 M NaOH
10.0	0.15 M H_3BO_3	0.125 M NaOH

EXPERIMENTAL

Reagents

The standard sample of NLT (99.0%, from Bristol Myers Squibb) was supplied from Novartis. The stock solution of NLT was prepared by the dissolution of precisely weighed 10 mg NLT in 10 mL methanol in order to have the concentration of 1 mg mL^{-1}. The stock solutions of model compounds diclofenac (dissolving in distilled water) and lidocaine (dissolving in distilled ethanol) were prepared through the same procedure. The pH solutions were prepared using Table 1. The stock solutions were diluted to the working concentration with the selected supporting electrolytes (10% methanol ratio was kept constant for NLT and Lidocaine). All supporting electrolyte solutions were prepared using analytical grade reagents and purified water from a Millipore Milli-Q system based on Table 1.

Apparatus

All the electrochemical studies were performed by using a computer-controlled Autolab potentiostat/galvanostat PGSTAT 302 with GPES 4.9 software. An electrochemical cell with a three-electrode configuration was used with a counter electrode as platinum wire, a GC working electrode (Bioanalytical Systems, West Lafayette, IN, USA; Ø: 1.6 mm, diameter) and saturated Ag/AgCl as reference electrode. pH measurements were carried out using a model 538 pH-meter (WTW, Weilheim, Germany) with an accuracy of ± 0.05 pH.

Differential pulse voltammograms presented in the manuscript were baseline corrected using the moving average peak width 0.002 with GPES 4.9 software.

CONCLUSIONS

The study of the redox behaviour of different organic compounds using electrochemical techniques can provide valuable insights into the biological redox reactions of these molecules.[20] The irreversible and diffusion-adsorption mix controlled electrochemical oxidation of NLT exhibited two main anodic peaks. The oxidation mechanism of NLT was proposed as the behaviour of first and second peak related to diphenylamine and acetamide moiety in molecule, respectively. The number of electrons in the rate-determining step was calculated as 2 for the first and second peaks. The rate constant and surface coverage coefficients were also calculated.

REFERENCES

1. S.A. Ozkan, "Electroanalytical methods in pharmaceutical analysis and their validation", HNB Pub., New York, 2011.
2. M.R. Smyth and J.G. Vos (Eds.) "Analytical Voltammetry", Vol. XXVII, Elsevier, Amsterdam, 1992.
3. V.S. Bagotsky (Ed.) "Fundamentals of electrochemistry", 2nd Ed., Wiley-Interscience Pub, USA, 2006.
4. J. Wang, "Electroanalytical techniques in clinical chemistry and laboratory medicine", VCH, New York, 1998.
5. R.N. Adams (Ed.) "Electrochemistry at solid electrodes", Marcel Dekker Inc., New York, 1969.
6. http://www.cancer.gov/cancertopics/druginfo/nilotinib
7. D. L. DeRemer, C. Ustun and K. Natarajan, *Clin. Ther.*, **2008**, *30*, 1956-1975.
8. S. Nadanaciva, S. Lu, D. F. Gebhard, B. A. Jessen, W. D. Pennie and Y. Will, *Toxicol. In Vitro*, **2011**, *25*, 715-723.
9. J.A. Bard and L.R. Faulkner, "Electrochemical methods: Fundamentals and applications", 2nd Ed., John Wiley & Sons, Inc., USA, 2001, p. 226-260.
10. A.D.R. Pontinha, S.M.A. Jorge, V.C. Diculescu, M. Vivan and A.M. Oliveira-Brett, *Electroanalysis*, **2012**, *24*, 917-923.
11. R.G. Compton and C.E. Banks, "Understanding Voltammetry", World Scientific, London, 2007.
12. D.K. Gosser, "Cyclic Voltammetry", VCH, New York, 1994.
13. R.S. Nicholson and I. Shain, *Anal. Chem.,* **1964***, 36*, 706-723.
14. F. Marken, A. Neudeck and A.M. Bond, "Cyclic voltammetry". In: F. Scholz (Ed.) "Electroanalytical methods", 2nd Ed. Springer, Berlin, 2010, p. 57-106.
15. E. Laviron, *J. Electroanal. Chem.*, **1979**, *101*, 19-28.
16. H. Lund and O. Hammerich, "Organic electrochemistry", 4th Ed., Marcel Dekker, New York, 2001.
17. J. Grimshaw, "Electrochemical reactions and mechanism in organic chemistry", Elsevier, New York, 2000.
18. R. T. S. Oliveira, G. R. Salazar-Banda, V. S. Ferreira, S. C. Oliveira and L.A. Avaca, *Electroanalysis*, **2007**, *19*, 1189-1194.
19. K. Srinivasan, K. Kayalvizhi, K. Sivakumar and T. Stalin, *Spectrochim. Acta A,* **2011**, *79*, 169- 178.
20. C.M.A. Brett and A.M. Oliveira Brett, "Electrochemistry: Principles, Methods and Applications", Oxford University Press, Oxford, 1993.